Structure factors of the unitary gas under supernova conditions

Andrei Alexandru,[1,2,*] Paulo F. Bedaque,[2,†] and Neill C. Warrington[2,‡]

[1]*Department of Physics, The George Washington University, Washington, DC 20052, USA*
[2]*Department of Physics, University of Maryland, College Park, Maryland 20742, USA*

We compute with lattice field theory the vector and axial static structure factors of the unitary gas for arbitrary temperature above the superfluid transition and for fugacities $0.1 < z < 1.0$. Using the lattice formulation, we calculate beyond the validity of the virial expansion, a commonly used technique in many-body physics. We find qualitative differences in the behavior of the structure factors at high fugacity compared to the predictions of the virial expansion. Due to the large scattering length of neutrons, we expect the unitary gas structure factors to approximate the structure factors of hot neutron gases, and we therefore expect our calculations to be useful in supernova simulations, where neutron gas structure factors are needed to compute in-medium neutrino-neutron scattering rates.

I. INTRODUCTION

The unitary gas, a gas of spin 1/2 fermion with short range interactions tuned so a two-body bound state exists at threshold, is a classic example of a conformal system. The challenge in studying it stems from the fact that it is a strongly coupled theory for which no perturbative method applies. At the same time, a number of physical systems in nature, varying over a large range of energy scales, are very close to being a unitary gas. Besides dilute atomic fermionic gases in atomic traps, the dilute and warm neutron gas, as found in core collapse supernova, is close to being a unitary gas. Indeed, the conditions required for a neutron gas to be close to the unitary gas is that the typical interparticle distance l should lie between the scattering length a and the range of the forces R, while, at the same time, the thermal wavelength λ_T should be larger than R, so that the details of the potential are not probed during collisions. For a neutron gas where the scattering length is $a \simeq -23$ fm and the range of the nuclear forces R set by the inverse pion mass, $R \approx 1/m_\pi \approx 1.3$ fm, the neutron gas will approximate well a unitary gas over the range of densities and temperatures $0.01n_0 \leqslant n \leqslant 0.1n_0$ ($n_0 \approx 0.16/$ fm^3 is the density of nuclear matter) and $T \leqslant 10$ MeV. This is similar to the range of densities and temperatures found in the neutrino sphere of core collapse supernovae [1–3], the region where neutrinos decouple from matter during the explosion, and which is essential to the modeling of the core collapse supernova process [4,5].

The interactions between the neutrinos and the neutron matter are controlled not only by the cross section of neutrinos scattering off individual neutrons, but also by many-body effects. As a particularly dramatic demonstration of this, recent three-dimensional (3D) supernova simulations have shown that small changes in the scattering rate, of the order that could be caused by in-medium effects [6], can turn a dud into an explosion. The in-medium differential scattering rate of neutrinos due to neutral current scattering processes in the elastic (zero energy transfer) approximation is given by [7]

$$\frac{d\Gamma}{d\cos\theta} = \frac{G_F^2 E_\nu^2}{4\pi^2} \left[c_V^2 (1 + \cos\theta) S_V(q) + c_A^2 (3 - \cos\theta) S_A(q) \right],$$
(1.1)

where E_ν is the energy of the neutrino, $\cos\theta$ is the scattering angle, and $q = 2E_\nu \sin\theta/2$ is the momentum transfer to the medium in which the neutrino is scattering. The functions $S_V(q)$ and $S_A(q)$ are the vector and axial static structure factors, respectively, and they encode the properties of the medium. In the non-relativistic limit relevant here,[1] the structure factors are defined as Fourier transforms of equal time correlation functions

$$S_V(q) = \int d^3x e^{-iq\cdot x} \langle \delta n(x, 0)\delta n(0, 0)\rangle,$$

$$S_A(q) = \int d^3x e^{-iq\cdot x} \langle \delta s_z(x, 0)\delta s_z(0, 0)\rangle,$$

where n is the density of particles, and s_z is the density of z component of spin. In a supernova, these structure factors are computed in a high temperature medium composed of

---

*aalexan@gwu.edu
†bedaque@umd.edu
‡ncwarrin@umd.edu

[1]The conditions of the neutrino sphere, $T \approx 5$–10 MeV and $n \approx 10^{-3}$–$10^{-1}n_0$ are such that the neutrons composing the medium can be approximated by a nonrelativistic spin-1/2 field. In the nonrelativistic limit, neutrinos couple to neutron density and spin.

primarily neutrons; we calculate here S_V and S_A in a hot medium composed of unitary fermions as a first step toward calculating the structure factors of the neutron gas.

Various properties of the unitary gas have been computed in the past, with particular interest in the low temperature regime. Thermodynamic functions in the have been calculated by several groups [8–13]. These calculations are done in the vicinity of the superfluid phase transition and in the postulated "pseudogap" regime, both of which occur at low temperature. The contact has also been calculated by several groups [14–17], and the vector static structure factor has been calculated by relatively fewer groups, with a zero temperature quantum Monte Carlo calculation performed in [18].

Due to the unique conditions of the neutrino sphere, we explore here a higher temperature regime than in previous studies; as a result we probe novel regions of parameter space of the unitary gas. Furthermore, we present here the first non-perturbative calculation of both the axial and vector structure factors of the unitary gas at the thermodynamic parameters found in the neutrino sphere. In particular, we calculate the structure factors of the unitary gas beyond the domain of validity of the commonly used virial expansion, which has been used to calculate structure factors perturbatively in the past [19].[2]

This paper is organized as follows. In Sec. II we describe the methods we used to numerically simulate the unitary gas. In Sec. III we describe how we tune lattice parameters of the Hamiltonian to satisfy the unitary condition. In Sec. IV we derive the observables of interest. In Sec. V we show the results of our lattice calculation and in Sec. VI we state our conclusions.

II. FORMALISM

We will use the following lattice Hamiltonian to describe the unitary gas:

$$H - \mu N = \underbrace{\sum_{\sigma;xy} \psi_{\sigma;x}^{\dagger} k_{xy} \psi_{\sigma;y}}_{K} \underbrace{-\mu \sum_{\sigma;x} \psi_{\sigma;x}^{\dagger} \psi_{\sigma;x} - \frac{G}{\Delta x^3} \sum_{x} \psi_{1;x}^{\dagger} \psi_{1;x} \psi_{2;x}^{\dagger} \psi_{2;x}}_{V} . \quad (2.1)$$

Here, $\psi_{\sigma;x}$ annihilates a fermion with spin σ at site x on a 3D spatial lattice, the fermionic fields are normalized such that $\{\psi_{\sigma;x}, \psi_{\sigma';x'}^{\dagger}\} = \delta_{\sigma\sigma'} \delta_{xx'}$ and the matrix k_{xy} is given by

$$k_{xy} = \frac{1}{2M \Delta x^2} \sum_{p} p^2 e^{-ip \cdot (x-y)}, \quad (2.2)$$

where p is a lattice momentum. The nonlocal hopping term generates the correct, continuum dispersion relation, instead of a lattice approximation that would be generated if a local hopping term had been used. The nonlocal structure of the Hamiltonian will not cause any difficulty in the simulations as this term is treated in momentum space. Of course, the hamiltonian in Eq. (2.1) is a discretized version of

$$H = \int d^3x \left[\psi_{\sigma}^{\dagger} \left(-\frac{\nabla^2}{2M} - \mu \right) \psi_{\sigma} - \frac{G}{2} (\psi_{\sigma}^{\dagger} \psi_{\sigma})^2 \right], \quad (2.3)$$

which, for a properly renormalized G, describes nonrelativistic fermions at unitarity. As we will show later, if we regularize the theory using the lattice discretization in Eq. (2.1), the unitarity point is given by $G \approx 5.14435 \Delta x/M$.

Our object of study is the partition function (and its derivatives with respect to local spacetime sources)

$$Z = \text{Tr}(e^{-\beta(H-\mu N)}) = \text{Tr} \left(\prod_{t=1}^{N_t} e^{-\Delta t K} e^{-\Delta t V} \right) + \mathcal{O}(\Delta t^2), \quad (2.4)$$

where $\Delta t = \beta/N_t$.[3] The numerical Monte Carlo method we will use is very similar to the one in [21,22]. The four-fermion interaction can be written in terms of fermion bilinears by noting that

$$e^{-\Delta t V} = \prod_{x} \exp \left(\Delta t \mu (n_{1x} + n_{2x}) + \frac{\Delta t G}{\Delta x^3} n_{1x} n_{2x} \right)$$

$$= \prod_{x} \frac{1}{f_0} \int dA_x e^{-\frac{1}{\hat{g}}(\cosh A_x - 1)} e^{(n_{1x} + n_{2x})(A_x + \hat{\mu})} \quad (2.5)$$

with $n_{\sigma} = \psi_{\sigma}^{\dagger} \psi_{\sigma}$, provided μ, G are related to $\hat{\mu}, \hat{g}$ through $e^{\mu \Delta t} = \frac{f_1}{f_0} e^{\hat{\mu}}$ and $e^{\frac{G \Delta t}{\Delta x^3}} = \frac{f_0 f_2}{f_1^2}$, where the functions $f(\hat{g})$ are

$$f_{\alpha}(\hat{g}) \equiv \int_{-\infty}^{\infty} dA \exp \left(-\frac{\cosh A - 1}{\hat{g}} + \alpha A \right). \quad (2.6)$$

Finally, using the identity

$$\text{Tr} \left(e^{-\sum \psi_x^{\dagger}(M_1)_{xy}\psi_y} e^{-\sum \psi_x^{\dagger}(M_2)_{xy}\psi_y} \cdots e^{-\sum \psi_x^{\dagger}(M_N)_{xy}\psi_y} \right)$$

$$= \det \left(\mathbf{1} + e^{-M_N} \cdots e^{-M_1} \right) \quad (2.7)$$

for fermionic operators $\psi_x^{\dagger}, \psi_y$, we see that

$$Z \approx \text{Tr} \left(\prod_{t=1}^{N_t} e^{-\Delta t K} e^{-\Delta t V} \right) = f_0^{-N_s N_t} \int DA \, e^{-S_g(A)} \det$$

$$\times [\mathbf{1} + e^{N_t \hat{\mu}} B^{-1} C(A_{N_t-1}) \cdots B^{-1} C(A_0)]^2, \quad (2.8)$$

---

[2]The virial expansion has also been used to compute *dynamic* properties of the unitary gas. For example the shear and bulk viscosities have very recently been computed in [20].

[3]That this trotterization is correct to $\mathcal{O}(\Delta t^2)$ can be seen by noting that $\text{Tr}(\prod_{t=1}^{N_t} e^{-\Delta t K} e^{-\Delta t V}) = \text{Tr}(\prod_{t=1}^{N_t} e^{-\frac{\Delta t}{2} K} e^{-\Delta t V} e^{-\frac{\Delta t}{2} K})$ by cyclicity of the trace.

where

$$B_{xx'} = \sum_p e^{-ip\cdot(x-x')}e^{\hat{\gamma}\frac{p^2}{2}}, \quad C(A_t)_{xx'} = \delta_{xx'}e^{A_{x,t}}, \quad \hat{\gamma} \equiv \frac{\Delta t}{M\Delta x^2},$$
(2.9)

N_s is the number of spatial sites, and $DA = \prod_{xt} dA_{xt}$.

The same partition function, up to a constant multiplicative factor, can also be derived from the path integral over the Euclidean lattice action:

$$S = \frac{1}{\hat{g}} \sum_{x,t} (\cosh(A_{x,t}) - 1) + \sum_{\sigma;x,y,t} \hat{\psi}^\dagger_{\sigma;x,t} B_{xy} \hat{\psi}_{\sigma;y,t}$$
$$- \sum_{\sigma;x,t} \hat{\psi}^\dagger_{\sigma;x,t+1} e^{A_{x,t}+\hat{\mu}} \hat{\psi}_{\sigma;x,t}$$
$$= \frac{1}{\hat{g}} \sum_{x,t} (\cosh(A_{x,t}) - 1) + \sum_{\sigma;xtx't'} \hat{\psi}^\dagger_{\sigma;x,t} D_{xtx't'} \hat{\psi}_{\sigma;x',t'},$$
(2.10)

where we define the fermion matrix $D_{xt,x't'} = B_{xx'}\delta_{tt'} - e^{A_{xt}+\hat{\mu}}\delta_{t+1t'}$ (we implement antiperiodic boundary conditions in time by taking $\delta_{N_t,N_{t-1}} \equiv -\delta_{0,N_{t-1}}$.) Indeed, the integration over Grassmann variables $\hat{\psi}$ leads to

$$\int DA D\hat{\psi} D\hat{\psi}^\dagger e^{-S[A,\psi^\dagger,\psi]} = \int DA e^{-S_g[A]} \det(D)^2, \quad (2.11)$$

where $S_g(A) \equiv \frac{1}{\hat{g}} \sum_{x,t} (\cosh(A_{x,t}) - 1)$ and D is the fermion matrix. The determinant $\det D$ can be written, by repeated use of the Schur complement identity, as

$$\det D = \det B^{N_t} \det [\mathbf{1} + e^{N_t\hat{\mu}} B^{-1} C(A_{N_t-1}) \ldots B^{-1} C(A_0)]$$
$$= \det (\mathbf{1} + U), \quad (2.12)$$

where $U \equiv e^{N_t\hat{\mu}} B^{-1} C(A_{N_t-1}) \ldots B^{-1} C(A_0)$. Therefore, the expression for the derived from the action Eq. (2.11) is equivalent to the one derived from the Hamiltonian in Eq. (2.8).

A few words about the Monte Carlo calculation of expression in Eq. (2.8) [or, equivalently, of expression Eq. (2.11)] are in order. First, since D is a real matrix $\det D$ is real, $\det D^2 \geqslant 0$ and the theory is sign-problem free. Second, the matrix B^{-1} is independent of A_{xt} and can be computed once at the beginning of the calculation and used thereafter. The matrices $C(A_t)_{xx'}$, which depend on A_{xt}, are diagonal and their multiplication has a computational cost of order $\mathcal{O}(N_s^2)$, where N_s is the number of spatial sites [instead of the $\mathcal{O}(N_s^3)$ cost for dense matrices]. Finally, we use the hybrid Monte Carlo algorithm of [23] to sample fields.

III. UNITARITY CONDITION

To obtain the unitary gas in the continuum and infinite volume limits, we tune the parameters of the lattice theory such that there is a zero energy two-particle bound state in the $^1S_0$ scattering channel at $\mu = 0$. The binding energy of the two-particle state can be determined from the position of the appropriate pole in the scattering amplitude. For this model, conservation of particle number allows us compute exactly the scattering amplitude by summing over all Feynman diagrams that contribute to two-particle scattering processes.

To compute the Feynman rules we start from the action Eq. (2.11), and integrate over the auxiliary fields:

$$\int_{-\infty}^{\infty} dA \exp\left(-\frac{\cosh A - 1}{\hat{g}}\right) \exp[-\hat{\psi}^\dagger e^{A+\hat{\mu}}\hat{\psi}]$$
$$= \int_{-\infty}^{\infty} dA \exp\left(-\frac{\cosh A - 1}{\hat{g}}\right)$$
$$\times \left[1 - \hat{\psi}^\dagger e^{A+\hat{\mu}}\hat{\psi} + \frac{1}{2}(\hat{\psi}^\dagger e^{A+\hat{\mu}}\hat{\psi})^2\right]$$
$$= f_0 - f_1 \hat{\psi}^\dagger e^{\hat{\mu}}\hat{\psi} + \frac{1}{2}f_2(\hat{\psi}^\dagger e^{\hat{\mu}}\hat{\psi})^2$$
$$= f_0 \exp\left[\frac{f_1}{f_0}\hat{\psi}^\dagger e^{\hat{\mu}}\hat{\psi} + \left(\frac{f_2}{f_0} - \frac{f_1^2}{f_0^2}\right)\frac{1}{2}(\hat{\psi}^\dagger e^{\hat{\mu}}\hat{\psi})^2\right]. \quad (3.1)$$

The action in terms of Grassmann variables is then

$$S_f = \sum_{\sigma;x,y,t} \psi^\dagger_{\sigma;x,t} B_{xy} \psi_{\sigma;y,t} - e^{\hat{\mu}}\frac{f_1}{f_0} \sum_{\sigma;x,t} \psi^\dagger_{\sigma;x,t+1} \psi_{\sigma;x,t} - e^{2\hat{\mu}}$$
$$\times \left(\frac{f_2}{f_0} - \frac{f_1^2}{f_0^2}\right) \sum_{x,t} \psi^\dagger_{1;x,t+1} \psi_{1;x,t} \psi^\dagger_{2;x,t+1} \psi_{2;x,t}. \quad (3.2)$$

For an infinite lattice in both space and time, the momentum space action reads

$$S_f = \int_{-\pi}^{\pi} d^4 p\, \psi^\dagger_\sigma(\omega,p)[e^{\hat{\gamma}\vec{p}\cdot\vec{p}/2} - e^{i\omega+\hat{\mu}+\ln f_1/f_0}]\psi_\sigma(\omega,p)$$
$$- e^{2\hat{\mu}}\left(\frac{f_2}{f_0} - \frac{f_1^2}{f_0^2}\right) \int_{-\pi}^{\pi} d^4 p_1 d^4 p_2 d^4 p_3 d^4 p_4\, \delta^4$$
$$\times (p_1 + p_3 - p_2 - p_4)e^{i\omega_1 + i\omega_3}$$
$$\times \psi^\dagger_1(p_1)\psi_1(p_2)\psi^\dagger_2(p_3)\psi_2(p_4), \quad (3.3)$$

leading to the Feynman rules in Fig. 1.

In terms of diagrams, the scattering amplitude is given by the sum of graphs shown in Fig. 2. Choosing kinematics $(E/2, \vec{p})$ and $(E/2, -\vec{p})$ on the external legs, the scattering amplitude has the analytic expression

$$-\mathcal{A} = \frac{1}{\left[e^{2\hat{\mu}}\left(\frac{f_2}{f_0} - \frac{f_1^2}{f_0^2}\right)e^{iE}\right]^{-1} - L(E)}, \quad (3.4)$$

where

$$L(E) = \int_{-\pi}^{\pi} \frac{dq_0}{2\pi} \int_{-\pi}^{\pi} \frac{d^3 q}{(2\pi)^3}$$
$$\times G(q_0 + E/2, \vec{q})G(-q_0 + E/2, -\vec{q}) \quad (3.5)$$

is the fermion-fermion loop iterated in the bubble sum. To work at $\mu = 0$, using the map derived above, we set $\hat{\mu} = \log\frac{f_0}{f_1}$ and the unitarity condition, that the amplitude has a pole at $E = 0$ at zero density, becomes

$$\frac{f_2 f_0}{f_1^2} - 1 = \frac{1}{L(0)} \quad \text{with} \quad L(0) = \int_{-\pi}^{\pi} \frac{d^3 q}{(2\pi)^3} \frac{1}{e^{\hat{\gamma}q^2} - 1}. \quad (3.6)$$

Given any $\hat{\gamma} = \Delta t/(M\Delta x^2)$, this condition fixes the lattice coupling $\hat{g}$. In principle we could enforce this condition for
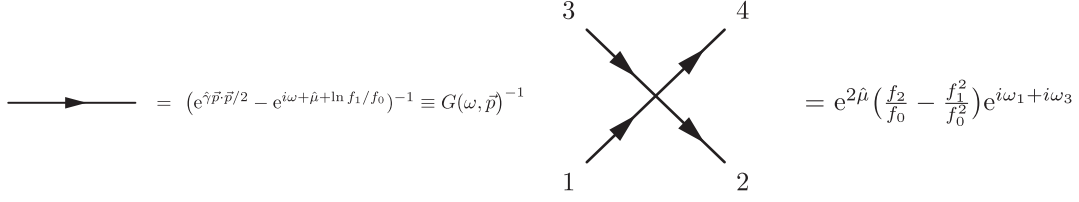
FIG. 1. Feynman rules corresponding to the action in Eq. (3.3) for propagator and vertex.

any value of Δx and Δt and then choose any sensible path to take the limit $\Delta t \to 0$, $\Delta x \to 0$. In practice we find it advantageous to fix Δx, fix G from the unitarity condition

$$\frac{MG}{\Delta x} = \lim_{\hat{\gamma} \to 0} \frac{1}{\hat{\gamma} L(0)} = 5.14435 \ldots, \quad (3.7)$$

and take the limit $\Delta t \to 0$ while $\hat{g}$ is fixed by $\frac{\Delta t G}{\Delta x^3} = \log(\frac{f_2 f_0}{f_1^2})$. This has the advantage that for fixed Δx, the discretized partition function has $\mathcal{O}(\Delta t^2)$ errors, since for this parameter choice the partition function derived from the action is the same as the approximation introduced in Eq. (2.4). This is the condition we use to fix couplings in Monte Carlo calculations. Of course, a subsequent spatial continuum limit $\Delta x \to 0$ is required to get the final results.

IV. OBSERVABLES

We compute three observables: the density, the vector structure factor, and the axial structure factor. The density is defined through the standard thermodynamic relation, and has the path integral expression

$$
\begin{aligned}
\langle n \rangle &= \frac{1}{V} \frac{\partial}{\partial \mu} (T \log Z) \\
&= \frac{1}{\Delta x^3} \frac{1}{N_s} \frac{1}{Z} \int DA e^{-S_g(A)} \det(\mathbf{1} + U(A))^2 \, \mathrm{Tr} \\
&\quad \times [\mathbf{1} - (\mathbf{1} + U(A))^{-1}] \\
&= \frac{1}{\Delta x^3} \frac{1}{N_s} \langle \mathrm{Tr}[\mathbf{1} - (\mathbf{1} + U)^{-1}] \rangle, \quad (4.1)
\end{aligned}
$$

where $U(A) = e^{N_t \hat{\mu}} B^{-1} C(A_{N_t - 1}) \ldots B^{-1} C(A_0)$. Our results are derived using cubic boxes with N_x sites in each dimension, so the total number of sites in a time slice is $N_s = N_x^3$. The vector and axial structure factors are defined as Fourier transforms of equal time correlation functions of the density

$n = n_1 + n_2$ and spin $s_z = n_1 - n_2$, respectively:

$$
\begin{aligned}
S_V(q) &= \sum_x \Delta x^3 e^{-iq \cdot x} \langle \delta n(x, 0) \delta n(0, 0) \rangle, \\
S_A(q) &= \sum_x \Delta x^3 e^{-iq \cdot x} \langle \delta s_z(x, 0) \delta s_z(0, 0) \rangle. \quad (4.2)
\end{aligned}
$$

Here, we have defined the Heisenberg operators

$$
\begin{aligned}
\delta n(x, t) &= n(x, t) - \langle n \rangle, \\
\delta s_z(x, t) &= s_z(x, t) - \langle s_z \rangle. \quad (4.3)
\end{aligned}
$$

It is possible to derive path integral expressions of $S_V(q)$ and $S_A(q)$ by taking derivatives with respect to local sources. Coupling the theory to a spacetime dependent source on the $t = 0$ time slice, then setting the source to a constant after taking derivatives, one derives the following path integral expressions:

$$
\begin{aligned}
\Delta x^6 &\langle n_1(x, 0) n_1(0, 0) \rangle \\
&= \frac{1}{Z} \int DA e^{-S_g(A)} \det(\mathbf{1} + U(A))^2 \\
&\quad \times [(\mathbf{1} - (\mathbf{1} + U(A))^{-1})_{00} (\mathbf{1} - (\mathbf{1} + U(A))^{-1})_{xx}] \\
&\quad + \frac{1}{Z} \int DA e^{-S_g(A)} \det(\mathbf{1} + U(A))^2 \\
&\quad \times [(\mathbf{1} - (\mathbf{1} + U(A))^{-1})_{0x} (\mathbf{1} + U(A))_{x0}^{-1}], \\
\Delta x^6 &\langle n_1(x, 0) n_2(0, 0) \rangle \\
&= \frac{1}{Z} \int DA e^{-S_g(A)} \det(\mathbf{1} + U(A))^2 \\
&\quad \times [(\mathbf{1} - (\mathbf{1} + U(A))^{-1})_{00} (\mathbf{1} - (\mathbf{1} + U(A))^{-1})_{xx}]. \quad (4.4)
\end{aligned}
$$

Since the action is invariant under $SU(2)$ spin rotations on the lattice (and in the continuum) $\langle n_1(x, 0) n_1(0, 0) \rangle = \langle n_2(x, 0) n_2(0, 0) \rangle$ and $\langle n_1(x, 0) n_2(0, 0) \rangle = \langle n_2(x, 0) n_1(0, 0) \rangle$, therefore the two correlation functions above are the only two
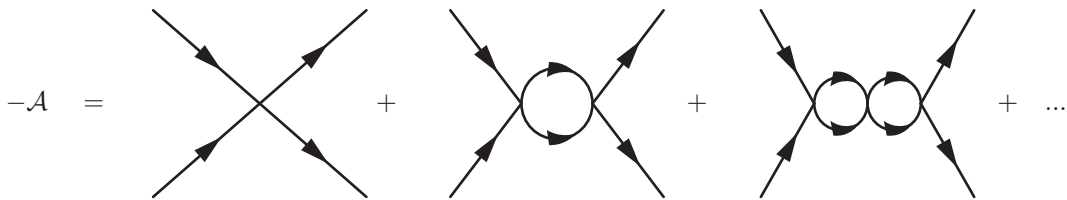

FIG. 2. The scattering amplitude $\mathcal{A}$ is given by the bubble sum above. To tune to unitarity on the lattice, we compute the bubble sum with lattice vertices and propagators on a lattice of infinite spacetime extent, corresponding to the zero temperature and infinite volume limits, and demand that there exist a zero energy bound state.

TABLE I. Three sets of parameters used in finite volume, space and time continuum extrapolations.

Volume extrapolation	Space continuum extrapolation	Time continuum extrapolation
$\Delta x = 0.4$, $\Delta t = 0.01$, $N_t = 40$, $N_x = 5, 7, 9$	$\Delta x = 0.4 \frac{5}{N_x}$, $\Delta t = 0.01$, $N_t = 40$, $N_x = 5, 7, 9$	$\Delta x = 0.4$, $N_x = 7$, $\Delta t = 0.01 \frac{40}{N_t}$, $N_t = 40$, $N_t = 40, 60, 80$

independent density-density correlation functions. We compute these in our lattice calculations, then form the necessary linear combinations to compute S_V and S_A. We also take advantage of translation invariance and hypercubic rotation invariance by summing over all such transformations in our calculation. This process reduces stochastic fluctuations of observables.

V. RESULTS

Since the interactions in a unitary gas do not have any scale (the scattering length is infinite) the static structure factors $S_{V,A}$ of the unitary gas are function of the momentum q, chemical potential μ, temperature T, and mass M. The dimensionless quantity $S_{V,A}/n$ (where n is the density of the system) is therefore a dimensionless function of only two variables

$$S_V(q)/\langle n \rangle = F_V\left(\frac{q}{q_T}, z\right),$$

$$S_A(q)/\langle n \rangle = F_A\left(\frac{q}{q_T}, z\right) \quad (5.1)$$

with $q_T = \sqrt{6MT}$ and $z = e^{\mu/T}$. The presence of a lattice introduces three unphysical scales, the finite volume and the lattice spacings Δt and Δx. However, we will demonstrate below that our calculations are performed at large enough volumes and small enough Δt, Δx that the dependence of $F_{V,A}$ on $q_T \Delta x$ and $T \Delta t$ can be neglected.

Since the supernova collapse simulations are an important motivation for our calculations, we will concentrate on a subset of parameters relevant for the neutrino propagation on the neutrino sphere, namely, densities in the range of $0.001 n_0 < n < 0.03 n_0$ (where n_0 is the density of nuclear matter) and $3 \, \text{MeV} < T < 10 \, \text{MeV}$, corresponding to fugacities in the $0.01 \lesssim z \lesssim 3$ range. This range of values is motivational only. A realistic evaluation of structure factors to be used in supernova modeling should include a more realistic neutron-neutron interaction (with a nonzero scattering length and effective range) as well as a small amount of protons and light nuclei. This corrections will be investigated in a future study.

In order to explore the uncertainties arising from the finite volume and lattice spacing employed in our calculations we first compute the structure factors for two values of the fugacity, $z = 0.1$ and $z = 1.0$ using three sets of parameters (and $M = 1$, $T = 4.13$) shown in Table I. We use lattices with odd number of points in the spatial direction because such lattices converge to the infinite volume limit faster than those with even number of sites. For nuclear astrophysics applications it is useful to think of the systems of units we use as corresponding to $\Delta x = 1 = 5 \, \text{fm}$, $M = 1 = 938 \, \text{MeV}$, $\Delta t =$

$0.01 = 1.19 \, \text{fm}$. The results we find are shown in Figs. 3 and 4. They show that the calculations performed on the smallest volume and coarsest lattices are already sufficient to determine the infinite volume and continuum results, within the statistical errors. The only exception are the results for the densest systems in our range ($z = 1.0$). Only the two finest lattice results for S_A ($\Delta x = 0.4 \times 5/7$, $0.4 \times 5/9$), agree well within the statistical uncertainties while the results S_V are different for all three values of Δx. Even in this case, however, signs of convergence are clear, with the difference between the $\Delta x = 0.4$ and $\Delta x = 0.4 \times 5/7$ results being much smaller than between $\Delta x = 0.4 \times 5/7$ and $\Delta x = 0.4 \times 5/9$. Due to this dependence on Δx, we assign a systematic uncertainty of 5% on the results for the vector structure factors at the largest values of z.

The asymptotic limit of the structure factors are known on general grounds:

$$S_V(q \to \infty) = S_A(q \to \infty) = n. \quad (5.2)$$

Since we are limited by the lattice cutoff to values of $q < \pi/\Delta x$ we can see that this limit is reached in less dense system ($z = 0.1$) but larger values of the momentum would be needed to verify it at more dense systems ($z = 1.0$), as can be seen on Fig. 5. In the same figure we compare our results to some known analytic results. The $S_{V,A}(q \to 0)$ limits are determined by thermodynamics

$$S_V(q \to 0) = T\left(\frac{\partial n}{\partial \mu}\right),$$

$$S_A(q \to 0) = T\left(\frac{\partial s}{\partial h}\right). \quad (5.3)$$

These have been computed up to fourth order in the virial expansion [1] and are shown in blue. The second and fourth order virial results are shown as small segments on the vertical axis. The second order in the virial expansion of a *free* gas can also be easily computed and is shown in Fig. 5 as a grey dotted line. Virial results for nonzero value of the momentum are not yet available. However, a calculation up to second order in z using a pseudopotential interaction (tuned to unitarity) and finite values of q is available [19] and shown as dashed lines in Fig. 5.[4] As expected, all virial calculations agree well with our data at small ($z \lesssim 0.5$) but differ significantly at larger values of z.

Finally, we have compared with a recent calculation by Jensen *et al.* [9] of the thermodynamics of the unitary gas,

---

[4]The main motivation of the calculation in [19] was the computation of *dynamical* structure factors which cannot be computed with Monte Carlo methods of the kind discussed in this paper.
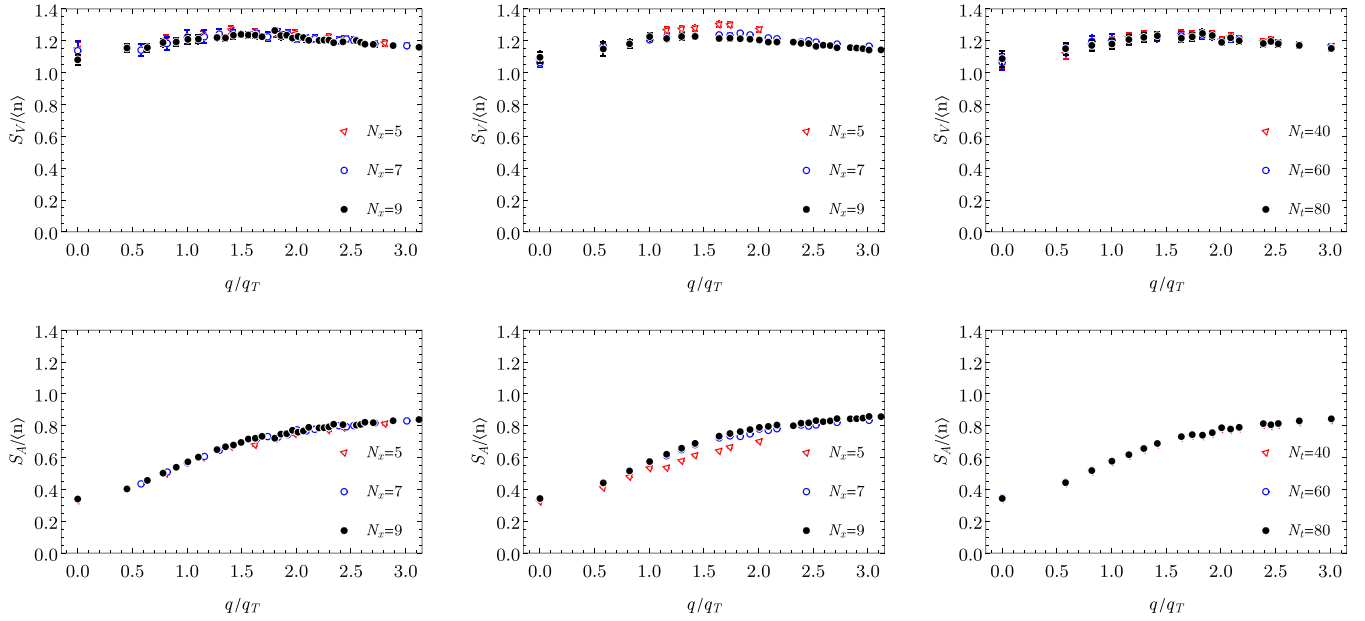
FIG. 3. Extrapolations of the vector (top row) and axial (bottom row) structure factors at $z = 1.0$. The first column are infinite volume limits, the second column is the $\Delta x \to 0$ limit and the last column is the $\Delta t \to 0$ limit. The structure factors vary little as the infinite volume and time continuum limit are taken. There is more variation of the structure factors as the spatial continuum limit is taken, however the the structure factors appear more or less converged on the finest lattice spacing.

including the $S_A(q \to 0)$ limit. The authors explore the parameter space $0.1 < T/T_F < 0.4$, where $T_F = (3\pi^2 n)^{2/3}/2M$. We extended our calculations to lower temperatures to be able to compare with their values. Jensen *et al.* report $S_A(q \to 0)/S_0 = 0.403(1)$ at $T/T_F = 0.353$ (where $S_0 = \frac{3n}{2}\frac{T}{T_F}$) on 9^3 lattices, while we obtain $S_A(q \to 0)/S_0 = 0.39(1)$ at $T/T_F = 0.371(5)$. Our results therefore appear consistent with those

of Jensen *et al.* Another calculation [13] reports values about 20% higher.

Our main results are summarized in Fig. 6. The error bar include the statistical errors but it should be kept in mind that an additional systematic for the vector structure factor reaching up 5% for the highest $z = 1.0$ should be added to the uncertainties.
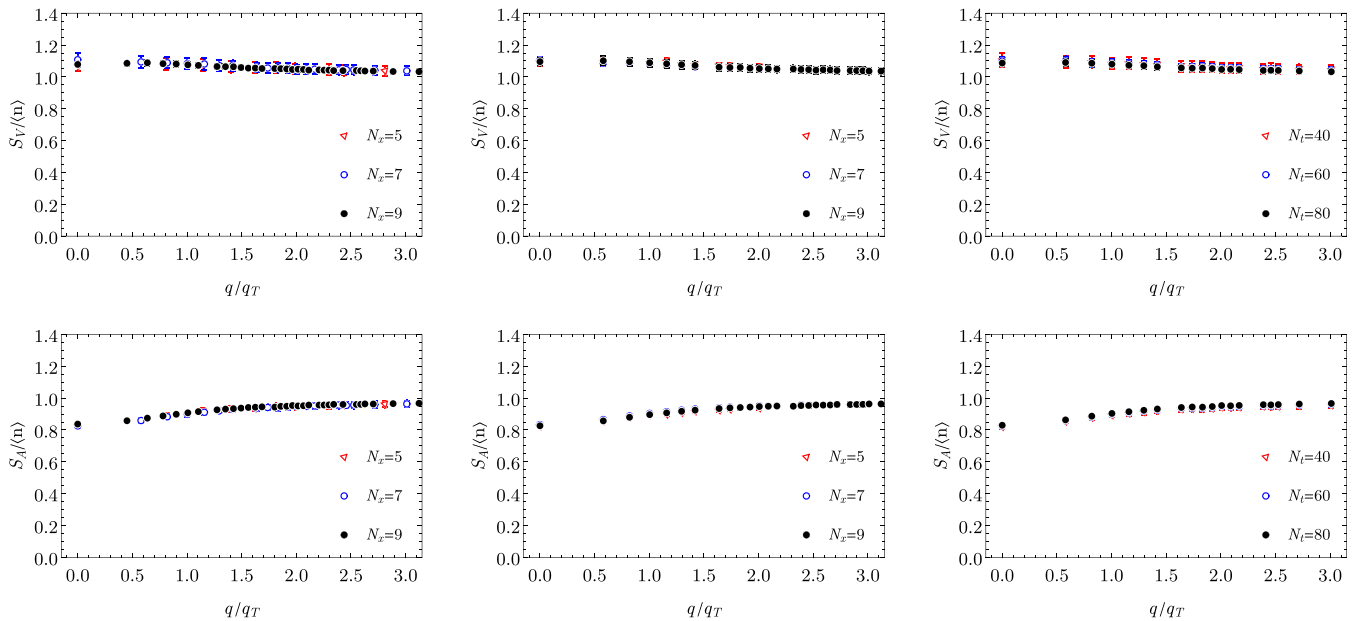

FIG. 4. Extrapolations of the vector (top row) and axial (bottom row) structure factors at $z = 0.1$. The first column are infinite volume limits, the second column is the $\Delta x \to 0$ limit and the last column is the $\Delta t \to 0$ limit. There is little variation in the structure factors for all three limits.
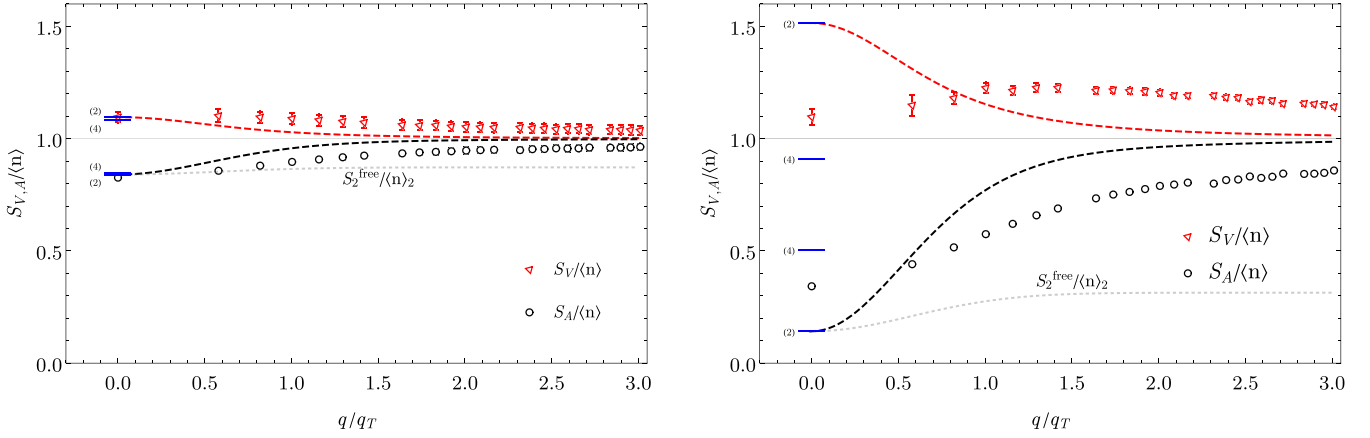
FIG. 5. Lattice results vs virial expansion calculations. We plot the scaled structure factors as a function of q/q_T for $z = 0.1$ (left) and $z = 1.0$ (right). The red data is the vector structure factor and the black is the axial structure factor. The dashed curves are calculations using a combination of the virial expansion to second order plus the pseudopotential method [19]. The dashed gray lines are the static structure factors computed in the free theory to $\mathcal{O}(z^2)$, scaled by the density computed to $\mathcal{O}(z^2)$. It is clear that, even at small z, interactions produce a sizable correction to the structure factors. The short horizontal bands in blue at small q/q_T are the various sum rules, calculated to $\mathcal{O}(z^2)$ and $\mathcal{O}(z^4)$ as discussed in the text. The horizontal line at $S_{V,A}(q)/\langle n \rangle = 1$ corresponds to the $q \to \infty$ limit derived from operator product expansion (OPE) [24].

VI. CONCLUSIONS

We computed the static structure factors of the unitary gas in the $0.6T_F \lesssim T \lesssim 6T_F$ using Monte Carlo methods, corresponding to fugacities in the $0.1 \lesssim z \lesssim 1.0$ range. The unitary gas at low densities is a reasonable model for a dilute neutron gas and this range of fugacities is the one relevant to the neutrino sphere (the region around a protoneutron star where neutrinos decouple) in core collapse supernova. The structure factors are the relevant many-body information to describe the interactions between the neutrinos and the neuron matter that drives the explosion. We compared our lattice calculations of the static structure factors with an $\mathcal{O}(z^2)$ calculation using the pseudopotential approach. We find reasonable agreement with the second order virial expansion at $z = 0.1$, while we find qualitative differences between the lattice and virial expansion at $z = 1.0$. In particular, the dramatic bump in the $\mathcal{O}(z^2)$ vector structure factor at small q/q_T is in fact not present.

We demonstrate that, for all densities explored, both the infinite volume and the $\Delta t \to 0$ limits are very well behaved, with negligible variation in both structure factors. At small density, the $\Delta x \to 0$ limit also yields negligible variation in the structure factors. At $z = 1.0$, the densest system we consider, we see some variation in the structure factors at the coarsest lattice spacings. We expect, however, that our calculations are within 5% of the exact result at our finest lattice spacing.

We also leave for future work an extension of this calculation to hot neutron matter that will require a more realistic interaction between neutrons, at least one leading to finite scattering lengths and non-zero effective range. We also leave for future work a more careful $\Delta x \to 0$ extrapolations. Such extrapolations require calculations on larger lattices, which are more expensive, but there is no fundamental difficulty in doing so.
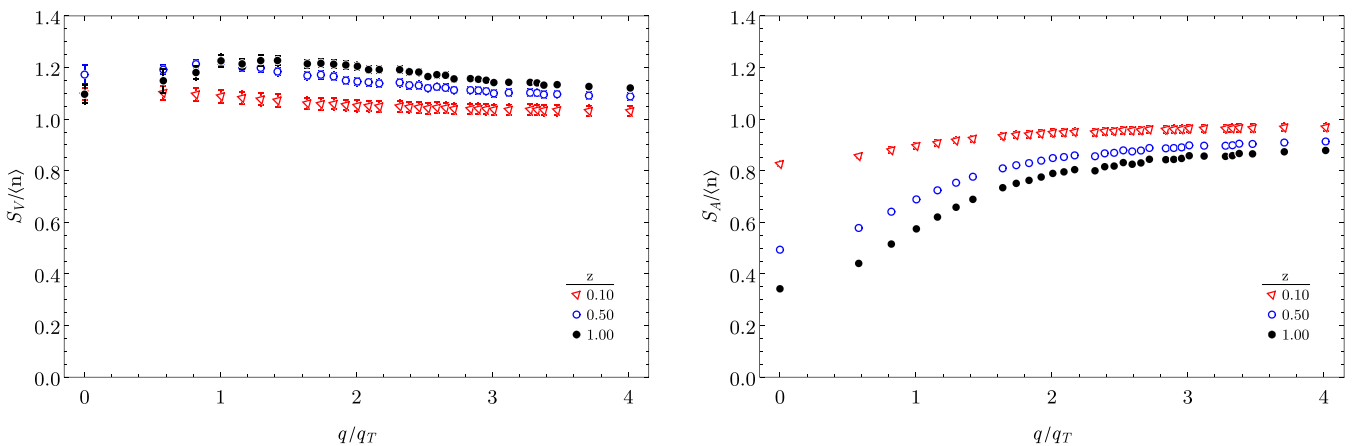

FIG. 6. Scaled structure factors for different fugacities as a function of the momentum in units of the thermal momentum q_T.

[1] Z. Lin and C. J. Horowitz, Phys. Rev. C **96**, 055804 (2017).

[2] C. J. Horowitz and A. Schwenk, Nucl. Phys. A **776**, 55 (2006).

[3] C. Horowitz and A. Schwenk, Phys. Lett. B **638**, 153 (2006).

[4] A. Burrows, Rev. Mod. Phys. **85**, 245 (2013).

[5] A. Mezzacappa, Annu. Rev. Nucl. Part. Sci. **55**, 467 (2005).

[6] T. Melson, H.-T. Janka, R. Bollig, F. Hanke, A. Marek, and B. Mueller, Astrophys. J. Lett. **808**, L42 (2015).

[7] C. Horowitz and A. Schwenk, Phys. Lett. B **642**, 326 (2006).

[8] C. N. Gilbreth and Y. Alhassid, Phys. Rev. A **88**, 063643 (2013).

[9] S. Jensen, C. N. Gilbreth, and Y. Alhassid, Phys. Rev. Lett. **124**, 090604 (2020).

[10] A. Bulgac, J. E. Drut, and P. Magierski, Phys. Rev. A **78**, 023625 (2008).

[11] J. E. Drut, T. A. Lähde, G. Wlazłowski, and P. Magierski, Phys. Rev. A **85**, 051601(R) (2012).

[12] P. Magierski, G. Wlazłowski, A. Bulgac, and J. E. Drut, Phys. Rev. Lett. **103**, 210403 (2009).

[13] G. Wlazłowski, P. Magierski, J. E. Drut, A. Bulgac, and K. J. Roche, Phys. Rev. Lett. **110**, 090401 (2013).

[14] S. Jensen, C. N. Gilbreth, and Y. Alhassid, (2019), arXiv:1906.10117 [cond-mat.quant-gas].

[15] J. E. Drut, T. A. Lähde, and T. Ten, Phys. Rev. Lett. **106**, 205302 (2011).

[16] O. Goulko and M. Wingate, Phys. Rev. A **93**, 053604 (2016).

[17] R. Rossi, T. Ohgoe, E. Kozik, N. Prokof'ev, B. Svistunov, K. Van Houcke, and F. Werner, Phys. Rev. Lett. **121**, 130406 (2018).

[18] S. Hoinka, M. Lingham, K. Fenech, H. Hu, C. J. Vale, J. E. Drut, and S. Gandolfi, Phys. Rev. Lett. **110**, 055305 (2013).

[19] P. F. Bedaque, S. Reddy, S. Sen, and N. C. Warrington, Phys. Rev. C **98**, 015802 (2018).

[20] J. Hofmann, Phys. Rev. A **101**, 013620 (2020).

[21] S. R. White, D. J. Scalapino, R. L. Sugar, E. Y. Loh, J. E. Gubernatis, and R. T. Scalettar, Phys. Rev. B **40**, 506 (1989).

[22] R. Blankenbecler, D. J. Scalapino, and R. L. Sugar, Phys. Rev. D **24**, 2278 (1981).

[23] A. Alexandru, P. F. Bedaque, and N. C. Warrington, Phys. Rev. D **98**, 054514 (2018).

[24] J. Hofmann and W. Zwerger, Phys. Rev. X **7**, 011022 (2017).